Vacancies mediated ordering in Ni-Mn-Ga shape memory alloys

D. Mérida [a], I. Unzueta [*,a], V. Sánchez-Alarcos [b,c], V. Recarte [b,c], J.I. Pérez-Landazábal [b,c], J.A. García [d], F. Plazaola [e]

[a] Applied Mathematics Department, University of the Basque Country UPV/EHU, Bilbao 48013, Spain
[b] Department of Science, Universidad Pública de Navarra, Campus de Arrosadía, Pamplona 31006, Spain
[c] Institute for Advanced Materials and Mathematics (INAMAT²), Universidad Pública de Navarra, Campus de Arrosadía, Pamplona 31006, Spain
[d] Department of Applied Physics II, University of the Basque Country UPV/EHU, Leioa 48940, Spain
[e] Department of Electricity and Electronics, University of the Basque Country UPV/EHU, Leioa 48940, Spain

ARTICLE INFO

ABSTRACT

Vacancy mediated diffusion is the main atomic mechanism that controls the ordering of substitutional alloys. In particular, in Ni-Mn-Ga shape memory alloys vacancies control the evolution of the $L2_1$ atomic order degree and consequently most of the order-dependent properties of the martensitic transformation. This work adapts a general phenomenological model to quantify the evolution of the vacancy concentration during the ordering process for three different Ni-Mn-Ga alloys. The results show that out of equilibrium vacancies are responsible of the ordering process, fixing the set of parameters governing it. The present work shows the suitability of the model to determine the vacancy dynamics throughout any process in which they intervene.

Diffusion processes and in particular atomic order play an important role in many materials of great technological interest [1–7]. Indeed, the different present phases in these materials have properties that depend strongly on the atomic order. In most cases, different thermo-mechanical treatments, such as quenching, ageing or mechanical deformations are used to modify the atomic order towards the tuning of the material properties [5,8,9]. Additionally, undesired phases controlled by diffusion processes may also affect the functional properties [10,11]. In this connection, the atomic diffusion, and the subsequent ordering is mediated by vacancies [12]. The works of Ren and Otsuka in Refs. [13,14] demonstrate the existing relation between short-range atomic order and diffusion of point defects, such as vacancies. Thus, a correct understanding of ordering processes and their relation to vacancy dynamics, which ultimately influence the diffusion processes, acquires key relevance towards the optimization of the multifunctional properties of materials.

The functional properties of Ni-Mn-Ga ferromagnetic shape memory alloys (FSMA) are related to the presence of a thermoelastic martensitic transformation (MT), which takes place between the austenite, a next nearest neighbors ordered cubic phase ($L2_1$ structure) and a less symmetric martensite phase. The MT temperature depends on the order degree of the $L2_1$ austenitic phase, and due to the displacive character of the MT, the atomic order degree is inherited by the martensitic phase

[15–20]. The vacancy mediated diffusion determines the atomic order degree, which is on the basis of the observed changes in MT characteristics [21–25]. This ordering process can be fulfilled by performing the so-called six-jump-cycle mechanism [12], which in the $L2_1$ structure, involves only Mn-Ni jumps in the first stage and Ga-Ni jumps in the second one [12]. However, up to now, it has not been possible to quantify the vacancy concentration during the complete ordering process, thus hindering a correct understanding of diffusion processes in Ni-Mn-Ga alloys.

Mérida et al. in Refs. [26,27], presented a phenomenological model in which the vacancy concentration was calculated throughout different heating-cooling cycles. The vacancy concentration measured after these cycles was found to be the same the one predicted by the model. This correspondence indicates that it is possible to determine the actual vacancy concentration at any given time/temperature during a certain thermal treatment. Thus, effectively, the proposed model should be valid to determine the concentration of vacancies throughout thermal treatments on time scales in which it is not possible to measure by standard techniques. That work paves the way for quantifying the vacancy concentration throughout any process in which they intervene (e. g., precipitation, phase-transitions, ...). Among those processes, this work will be focused on ordering dynamics. Based on the prior knowledge of vacancy kinetics, the initial model will be adapted to determine

* Corresponding author.
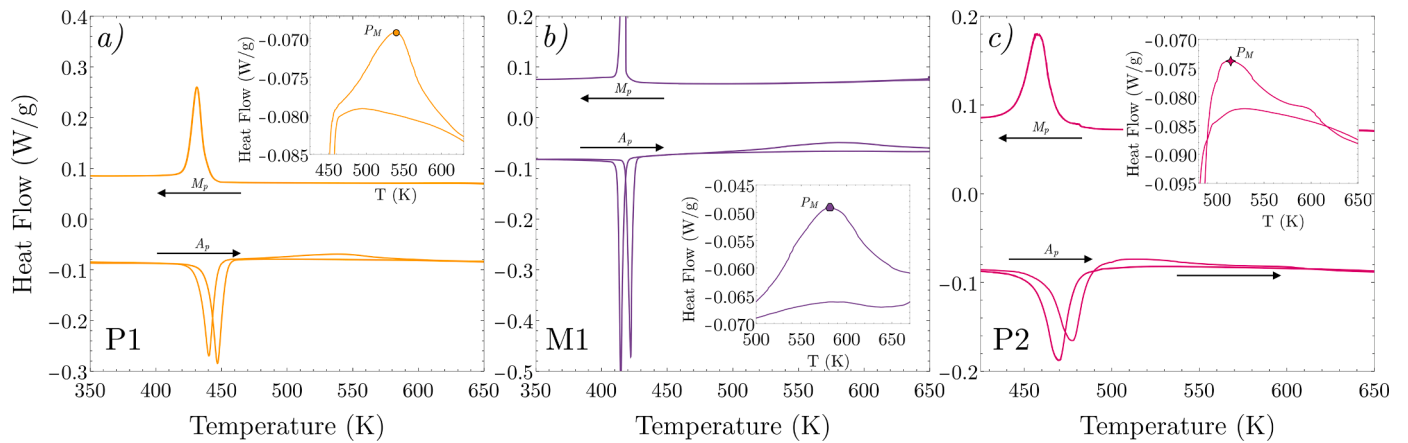*E-mail address:* iraultza.unzueta@ehu.eus (I. Unzueta).

Fig. 1. DSC thermogram of the (*a*) P1, (*b*) M1 and (*c*) P2 samples, quenched from 1173 K, and after a heating-cooling cycle. Each inset show the detail of the exothermic peak for each sample.

the vacancy concentration during the ordering process in Ni-Mn-Ga alloys. Combining Differential Scanning Calorimetric (DSC) measurements and the prediction of the model, a clear relation between ordering process and vacancy dynamics will be demonstrated.

In the present work two polycrystalline alloys with different compositions, $Ni_{51}Mn_{30}Ga_{19}$ at% (P1 alloy) and $Ni_{53}Mn_{26}Ga_{21}$ at% (P2 alloy) have been used. In addition, a single crystal sample (hereafter referred to as M1 alloy, $Ni_{50.5}Mn_{30.4}Ga_{19.1}$ at%) of a very similar composition to that of the P1 alloy, have also been investigated. The polycrystalline ingots of P1 and P2 samples were prepared from high purity elements by arc melting under protective argon atmosphere and then homogenized in evacuated quartz ampoules at 1173 K during 24 h [26]. In order to modify the atomic order-degree of the studied samples, they were subjected to quenching treatments. As a result, Ni-Mn-Ga samples quenched from high temperature show an exothermic peak during the first heating run in DSC measurements, located at higher temperatures than that of the MT. The fact that this peak fades away after the first heating run, points out the irreversible character of the process, which is related to recovery of the atomic disorder induced by quenching [16]. Thus, the ordering process has been monitored by tracking the evolution of the exothermic peak revealed by DSC measurements.

Small samples for DSC measurements were obtained from discs previously cut from the center of the ingots by slow speed diamond saw. The single crystal M1 sample was supplied by Goodfellow. Samples were quenched from 1173 K into ice water in a vertical furnace [26]. DSC measurements were carried out in a TA Q100 DSC instrument to study the thermal behavior of the alloys at a heating/cooling rate of 10 K/min. The samples were polished after quenching in order to ensure a good thermal contact with the equipment. All DSC measurements were performed under nitrogen atmosphere. The results of the initial characterization of the three studied samples are summarized in Table 1. The parameters governing the vacancy dynamics of P1, P2 and M1 samples have been obtained from Refs. [26,27].

The time evolution of the vacancy concentration out of equilibrium, $C_v(t)$, at a temperature T can be calculated by Damask and Dienes [28]:

$$\frac{dC_v(t)}{dt} = -\frac{\Gamma_0}{n}\left(C_v(t) - C_{eq}\right)\exp\left(-\frac{E_M}{k_B T}\right) \quad (1)$$

Here, $C_{eq} = \exp(S_v/k_B) \times \exp(-E_F/(k_B T))$ is the equilibrium vacancy concentration at temperature T. $\Gamma = \Gamma_0\exp(-E_M/k_B T)$ represents the jumping frequency of vacancies, where n is the average number of jumps a vacancy has to undertake before it becomes annihilated at a sink, S_v/k_B is the entropic factor of vacancy formation, k_B is the Boltzmann constant and E_F and E_M are the vacancy formation and migration energies, respectively. For a constant heating-cooling rate β, $dT/dt = -\beta$, the Eq. (1) can be rewritten as:
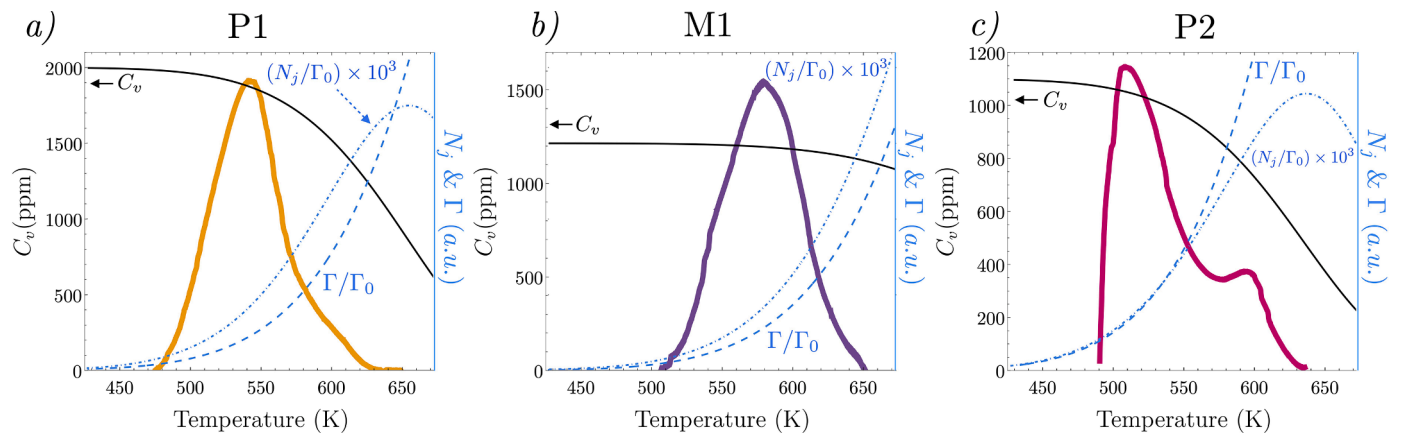

Fig. 2. Left axis: vacancy concentration $C_v(T)$ as a function of temperature (solid line) calculated using the parameters in Table 1 by means of Eqs. (1), (2) for (*a*) P1, (*b*) M1 y (*c*) P2 samples, for a constant heating rate of $\beta = 10$ K/min. The corresponding exothermic peak (bold-solid line) is shown for the sake of comparison between the calculated parameters. Right axis: scaled vacancy mediated diffusivity N_j/Γ_0, (dashed line) and the relative vacancy jumping frequency Γ/Γ_0 (dashed-dotted line), for each samples.

Table 1

Composition, martensitic reverse (A_p) and forward (M_p) transformation temperatures, and the temperature of the maximum of the exothermic peak (P_M) of the studied P1, P2 and M1 alloys (see Fig. 1). The last five rows summarize the experimental values of the migration and formation energy (E_M and E_F), n /Γ_0, S_v/k_B and the initial vacancy concentration C_0 used to evaluate Eq. (2), obtained from Refs. [27].

	Samples		
	P1	P2	M1
Ni(%at)	51	53	50.5
Mn(%at)	30	26	30.4
Ga(%at)	19	21	19.1
A_p (K)	447	470	427
M_p (K)	431	458	419
P_M (K)	543	508	580
E_M (eV)	0.60(3)	0.55(5)	0.63(3)
E_F (eV)	1.01(3)	0.90(7)	1.01(6)
n / $\Gamma_0(10^{-3}\text{s})$	9(1)	17(7)	50(15)
S_v /k_B (eV)	5.9(4)	4(1)	6.2(9)
C_0 (ppm)	2000(400)	1100(200)	1500(700)

$$\frac{dC_v(T)}{dT} = \left(C_v(T) - \exp\left(\frac{S_v}{k_B}\right)\exp\left(-\frac{E_F}{k_BT}\right)\right) \\ \left(\frac{\Gamma_0}{\beta \cdot n}\right)\exp\left(-\frac{E_M}{k_BT}\right) \tag{2}$$

For a general heat-treatment, the vacancy concentration has to be calculated using Eq. (1), but a for thermal treatment with a constant heating rate β, $C_v(T)$ can be calculated by integrating Eq. (2). However, the initial vacancy concentration (C_0) and the values of, n /Γ_0, S_v /k_B, E_F and E_M quantities have to be known in advance in order to determine the theoretical evolution of the vacancy concentration for a given thermal history. On the other hand, vacancy mediated diffusivity D_v, is proportional to the overall number of jumps the vacancies undertake, $D_v \propto N_j$. In turn, N_j is the product of the vacancy concentration and the vacancy jumping frequency at a given temperature [28]:

$$N_j = C_v(T) \times \Gamma = C_v(T) \times \Gamma_0 \exp\left(-\frac{E_M}{k_BT}\right). \tag{3}$$

As will be shown, the N_j parameter is relevant to understand the ordering created by vacancies during diffusion, which gives an idea of the ability/capacity of vacancies to order the sample at a given temperature.

Figure 1 shows the DSC thermograms obtained for (*a*) P1, (*b*) M1 and (*c*) P2 samples after quenching from 1173 K during two heating-cooling runs. The mayor exothermic and endothermic peaks correspond to the forward (M_p) and reverse (A_p) MT, respectively (see exact values in Table 1). In addition, during the second heating run the reverse MT temperature varies for all samples as it is evinced by the shift of A_p peaks. The ordering process taking place during the exothermic peak, enhances the $L2_1$ atomic order, and therefore the MT temperature changes between the subsequent heating runs [16]. In this connection, and as shown in the upper inset of each samples' figure, at temperatures above MT, an exothermic peak appears only in the first heating cycle for P1, P2 and M1 alloys, highlighting its irreversible nature.

In order to understand the vacancy dynamics during the ordering process (evinced by the exothermic peaks, see insets in Fig. 1), $C_v(T)$ and $N_j(T)$ are calculated by means of Eqs. (2), (3) along the same thermal history used in DSC measurements ($\beta = 10$ K/min). These equations are evaluated with the main parameters governing vacancy dynamics of the studied samples (see values in Table 1). It is important to notice that the experimental determination of $C_v(T)$ throughout the entire heating ramp is not possible by means of standard experimental techniques ($\sim$ 1h for PALS experiments at each T) in such a short time-scales.

Figure 2 (a–c) shows DSC exothermic peaks after base line

subtraction and normalization (bold-solid line). The position of the maximum of the exothermic process P_M varies with both composition and crystallinity of the alloy, where shifts up to $\sim$ 70 K are observed. Along with it, the calculated temperature dependence of the vacancy concentration $C_v(T)$ (solid line), the relative jumping frequency, Γ/Γ_0 (dashed line) and the N_j/Γ_0 (dashed-dotted line, which is proportional to vacancy mediated diffusivity), for P1, P2 and M1 samples are shown, respectively. It is important to notice that although N_j is related to both the amount of out of equilibrium vacancies and with those in thermal equilibrium at the corresponding temperature (C_{eq}), in quenched samples C_{eq} is much lower than the out of equilibrium vacancies, thus $C_{eq} \ll C_v$. As an example, at the highest temperature reached during the thermal cycling (673 K), $C_{eq} \approx 10$ ppm for all cases, which is much less than the $C_v(673K)$, which lies above 200 ppm.

The behavior of both, calculated vacancy dynamics and ordering peaks is different for the three studied samples. During the initial stages of the ordering process (between 450 - 550 K), C_v diminishes slowly. At increasing temperatures, the vacancy concentration reduces progressively in polycrystalline alloys but remains at high values in the single crystal sample M1. In both polycrystalline samples, the reduction in the vacancy concentration in the whole temperature range of the exothermic peak is $\approx 60 - 70\%$. On the other hand, for the single crystal M1 sample, the reduction is around of 15%. This difference in the evolution of the vacancy annihilation is linked to the fact that in polycrystals the mean distance that a vacancy has to undertake until it is annihilated at a grain boundaries is much less than in the single crystal. This fact is reflected by the value of the parameter n/Γ_0 (see Table 1), which is much higher for the monocrystalline M1 sample comparing with that of P1 sample.

On the other hand, the N_j parameter is proportional to vacancy concentration and the jumping frequency Γ (see Eq. (3). Therefore, it accounts for the rate at which the ordering process occurs. The vacancy concentration diminishes slowly during the temperature range of the exothermic peak, but the jumping frequency Γ increases according to the Boltzmann distribution function. Therefore, the total number of vacancy jumps N_j, will evolve in balance with those two magnitudes. As shown in Fig. 2, N_j increases monotonically during the temperature interval at which the ordering process takes place for P1, P2 and M1 samples. C_v decrease is compensated with the increase of the jumping frequency, which increases the ordering capacity of the remaining vacancies.

In contrast to the single crystal sample, in P1 and P2 samples N_j reaches a maximum at a particular temperature, well above the temperature range where the ordering process takes place, see Fig. 2(a,c). It marks the point at which the reduction in the vacancy concentration cannot be compensated by the jumping frequency Γ factor (see Eq. (3)). Therefore, the ordering capacity decreases above that temperature. In the case of the M1 single crystal sample N_j does not reach a maximum within the studied temperature range, because the decrease on C_v is too small to compete with the increase on jumping frequency. This is directly related with the large number of jumps that vacancies must undertake to reach a sink, which hampers their annihilation. Note that this sample has a n/Γ_0 value, at least, five times larger than the similar composition polycrystalline P1 sample (see Table 1). This maximum is of great interest, since it shows the temperature at which the ordering capacity is the largest. Above that temperature, the ordering capacity of vacancies decreases. However, in the particular cases of P1, M1 and P2 samples, this reduction of N_j does not affect the ordering process which is almost completed below the maximum of N_j. Anyway, in other intermetallic systems this maximum and the ordering process may overlap, affecting the capability of vacancies to complete the ordering process.

On the other hand, the lowest calculated vacancy concentration during the ordering process corresponds to P2 sample at 673 K with a value of 222 ppm. At this temperature, the equilibrium vacancy concentration for the three samples is around 10 ppm. Thus, it can be
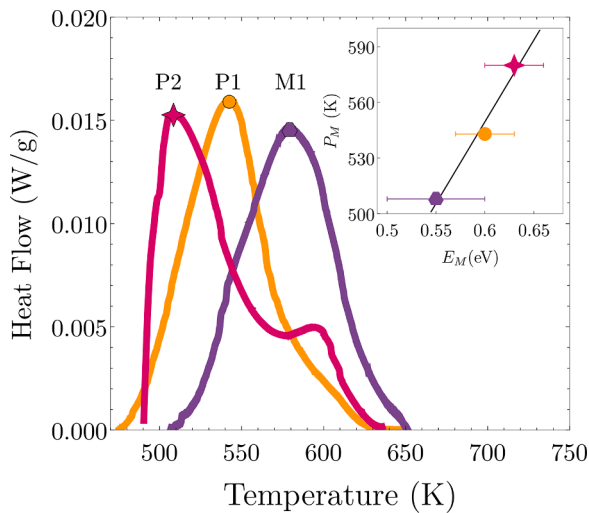
Fig. 3. The exothermic peaks of DSC thermograms for the P1, M1 and P2 samples after base line subtraction and normalization. The inset shows the mutual relationship between the maximum of the exothermic peak P_M and the E_M. The line is a guide to the eye.

concluded that $C_v \gg C_{eq}$, and therefore the parameters used for the calculation of the equilibrium vacancy concentration (E_F and S_v) have little impact. When $C_v \gg C_{eq}$, Eq. (2) reads:

$$\frac{dC_v(T)}{dT} = C_v(T) \left(\frac{\Gamma_0}{\beta \cdot n} \right) \exp \left(-\frac{E_M}{k_B T} \right) \tag{4}$$

The factor n/Γ_0, which affects the rate of reduction of the vacancy concentration (see Eq. (2)), also affects N_j through C_v (see Eq. (3)). However, in the present case C_v changes slowly along the exothermic peak or during the ordering process, while Γ varies by several orders of magnitude. As a result, in the three samples, n/Γ_0 has little effect in the vacancy mediated diffusivity N_j, and the latter is mainly influenced by the migration energy as defined in Eq. (3). Therefore, it can be concluded that the ordering process is mainly mediated by quenched-in vacancies, and among the five parameters used to characterize the vacancy dynamics presented in Ref. [27], C_0 and E_M become the most significant ones to analyze the ordering process in Ni-Mn-Ga samples.

Regarding C_0, by comparing the calculated positron lifetime values associated with Ni vacancies reported in Ref. [29], and the experimental values obtained from quenched Ni-Mn-Ga alloys in Refs. [26,27], it can be concluded that the ordering process is assisted by Ni vacancies. The small differences on C_0 observed between different samples can be also due to the specific characteristics of the structural configuration of the samples, like grain size, dislocations, internal stresses and other defects that restrict vacancy mobility.

On the other hand, P_M is directly correlated with the value of the vacancy migration energy E_M. Figure 3 compares the exothermic peaks and the inset shows the temperature of the maximum of the exothermic peak P_M as a function of the measured vacancy migration energy for P1, M1 and P2 samples. P2 sample has the lowest migration energy and so, its exothermic peak takes place at the lowest temperature, P1 has an intermediate value between the three samples and M1 shows the highest migration energy and consequently the exothermic peak occurs at the highest temperature. This mutual relationship evidences that the migration energy of Ni vacancies is one of the key parameters which govern the atomic ordering process in these samples.

In the present work, a model has been used to quantify the vacancy dynamics during the ordering process in three Ni-Mn-Ga samples. The results demonstrate that quenched-in vacancies (and not thermal equilibrium ones) play the fundamental role in atomic ordering in Ni-Mn-Ga alloys. The vacancy concentration retained during quenching is two orders of magnitude larger than the equilibrium concentration at tem-

peratures corresponding to the ordering process, C_{eq} (673 K) = 10 ppm $\ll C_v$ (673 K) = 200 ppm. In this context, vacancy formation energy E_F and its entropic factor S_v/k_B, are not so essential for vacancy mediated ordering processes. Besides, during the ordering process, C_v shows a small variation and n/Γ_0 affects little the diffusivity. Therefore, from the point of view of diffusivity the main influence on the ordering process comes from the initial vacancy concentration C_0 and its migration energy E_M.

Funding

Declaration of Competing Interest

The authors declare that they have no known competing financial interests or personal relationships that could have appeared to influence the work reported in this paper.

References

[1] K. Ullakko, J. Huang, V. Kokorin, R. O'Handley, Scr. Mater. 36 (1997) 1133, https://doi.org/10.1016/S1359-6462(96)00483-6.

[2] J. Tellinen, I. Suorsa, A. Jääskeläinen, I. Aaltio, K. Ullakko, A. Ltd. Proc. of 8th Int. Conf. on Actuator, 2002, p. 566.

[3] H. Bernas, J.-P. Attané, K.-H. Heinig, D. Halley, D. Ravelosona, A. Marty, P. Auric, C. Chappert, Y. Samson, Phys. Rev. Lett. 91 (2003) 077203, https://doi.org/10.1103/PhysRevLett.91.077203.

[4] P. Hu, H.b. Yang, D.a. Pan, H. Wang, J.j. Tian, S.g. Zhang, X.f. Wang, A. A. Volinsky, J. Magn. Magn. Mater. 322 (2010) 173, https://doi.org/10.1016/j.jmmm.2009.09.002.

[5] P. Neibecker, M. Leitner, G. Benka, W. Petry, Appl. Phys. Lett. 105 (2014) 261904, https://doi.org/10.1063/1.4905223.

[6] A. A. Emdadi, J. Cifre, O. Y. Dementeva, I. S. Golovin, J. Alloys Compd. 619 (2015) 58, https://doi.org/10.1016/j.jallcom.2014.08.231.

[7] I. Unzueta, D.A.d. R-Lorente, E. Cesari, V. Sánchez-Alarcos, V. Recarte, J. I. Pérez-Landazábal, J. A. García, F. Plazaola, Phys. Rev. Lett. 122 (2019) 165701, https://doi.org/10.1103/PhysRevLett.122.165701.

[8] Ş.N. Balo, N. Sel, Thermochim. Acta 536 (2012) 1, https://doi.org/10.1016/j.tca.2012.02.007.

[9] A. Nespoli, C. A. Biffi, E. Villa, A. Tuissi, J. Alloys Compd. 690 (2017) 478, https://doi.org/10.1016/j.jallcom.2016.08.143.

[10] M. Gojić, L. Vrsalović, S. Kožuh, A. Kneissl, I. Anžel, S. Gudić, B. Kosec, M. Kliškić, J. Alloys Compd. 509 (2011) 9782, https://doi.org/10.1016/j.jallcom.2011.07.107.

[11] Y.-J. Bai, X. Xu, Y. Liu, L.m. Xiao, G. L. Geng, Mater. Sci. Eng. A 334 (2002) 49, https://doi.org/10.1016/S0921-5093(01)01761-0.

[12] G. Erdélyi, H. Mehrer, A. Imre, T. Lograsso, D. Schlagel, Intermetallics 15 (2007) 1078, https://doi.org/10.1016/j.intermet.2007.01.001.

[13] X. Ren, K. Otsuka, Phys. Rev. Lett. 85 (2000) 1016, https://doi.org/10.1103/PhysRevLett.85.1016.

[14] X. Ren, K. Otsuka, Nature 389 (1997) 579, https://doi.org/10.1038/39277.

[15] M. L. Richard, J. Feuchtwanger, S. M. Allen, R. C. O'handley, P. Lázpita, J. M. Barandiaran, J. Gutierrez, B. Ouladdiaf, C. Mondelli, T. Lograsso, D. Schlagel, Philos. Mag. 87 (2007) 3437, https://doi.org/10.1080/14786430701297582.

[16] V. Sánchez-Alarcos, V. Recarte, J. Pérez-Landazábal, G. Cuello, Acta Mater. 55 (2007) 3883, https://doi.org/10.1016/j.actamat.2007.03.001.

[17] J. Gutiérrez, P. Lázpita, J. Barandiarán, M. Fdez-Gubieda, J. Chaboy, N. Kawamura, J. Magn. Magn. Mater. 316 (2007) e610, https://doi.org/10.1016/j.jmmm.2007.03.043.Proceedings of the Joint European Magnetic Symposia

[18] J. Chaboy, P. Lázpita, J. M. Barandiarán, J. Gutiérrez, M. L. Fernández-Gubieda, N. Kawamura, J. Phys. 21 (2008) 016002, https://doi.org/10.1088/0953-8984/21/1/016002.

[19] V. Sánchez-Alarcos, J. I. Pérez-Landazábal, V. Recarte, J. A. Rodríguez-Velamazán, V. A. Chernenko, J. Phys. 22 (2010) 166001, https://doi.org/10.1088/0953-8984/22/16/166001.

[20] C. Seguí, J. Pons, E. Cesari, Acta Mater. 55 (2007) 1649, https://doi.org/10.1016/j.actamat.2006.10.025.

[21] R. Santamarta, E. Cesari, J. Font, J. Muntasell, J. Pons, J. Dutkiewicz, Scr. Mater. 54 (2006) 1985, https://doi.org/10.1016/j.scriptamat.2006.03.018.

[22] Y. Zhang, L. Zhang, Q. Zheng, X. Zheng, M. Li, J. Du, A. Yan, Sci. Rep. 5 (2015) 11010EP, https://doi.org/10.1038/srep11010.

[23] Z.n. Zhou, L. Yang, J.g. Wang, T. Jin, Y. Huang, J. Li, Q. Hu, J.g. Li, Prog. Nat. Sci-Mater. 27 (2017) 356, https://doi.org/10.1016/j.pnsc.2017.04.012.

[24] S. Kustov, J. Pons, E. Cesari, J. V. Humbeeck, Acta Mater. 52 (2004) 3075, https://doi.org/10.1016/j.actamat.2004.03.009.

[25] S. Kustov, J. Pons, E. Cesari, J. V. Humbeeck, Acta Mater. 52 (2004) 3083, https://doi.org/10.1016/j.actamat.2004.03.010.

[26] D. Merida, J. A. García, V. Sánchez-Alarcos, J. I. Pérez-Landazábal, V. Recarte, F. Plazaola, Appl. Phys. Lett. 104 (2014) 231905, https://doi.org/10.1063/1.4882903.

[27] D. Merida, J. García, V. Sánchez-Alarcos, J. Pérez-Landazábal, V. Recarte, F. Plazaola, J. Alloys Compd. 639 (2015) 180, https://doi.org/10.1016/j.jallcom.2015.03.151.

[28] A. Damask, G. Dienes, Point Defects in Metals, Gordon and Breach, 1971.

[29] I. Unzueta, V. Sánchez-Alarcos, V. Recarte, J. I. Pérez-Landazábal, N. Zabala, J. A. García, F. Plazaola, Phys. Rev. B 99 (2019) 064108, https://doi.org/10.1103/PhysRevB.99.064108.